Circulation

ORIGINAL RESEARCH ARTICLE

Autoimmune Atrial Fibrillation

Ange Maguy, PhD; Yuvaraj Mahendran, PhD; Jean-Claude Tardif, MD; David Busseuil, PhD; Jin Li, MD

BACKGROUND: Atrial fibrillation (AF) is by far the most common cardiac arrhythmia. In about 3% of individuals, AF develops as a primary disorder without any identifiable trigger (idiopathic or historically termed lone AF). In line with the emerging field of autoantibody-related cardiac arrhythmias, the objective of this study was to explore whether autoantibodies targeting cardiac ion channels can underlie unexplained AF.

METHODS: Peptide microarray was used to screen patient samples for autoantibodies. We compared patients with unexplained AF (n=37 pre-existent AF; n=14 incident AF on follow-up) to age- and sex-matched controls (n=37). Electrophysiological properties of the identified autoantibody were then tested in vitro with the patch clamp technique and in vivo with an experimental mouse model of immunization.

RESULTS: A common autoantibody response against $K_{ir}3.4$ protein was detected in patients with AF and even before the development of clinically apparent AF. $K_{ir}3.4$ protein forms a heterotetramer that underlies the cardiac acetylcholine-activated inwardly rectifying K^+ current, I_{KACh}. Functional studies on human induced pluripotent stem cell–derived atrial cardiomyocytes showed that anti-$K_{ir}3.4$ IgG purified from patients with AF shortened action potentials and enhanced the constitutive form of I_{KACh}, both key mediators of AF. To establish a causal relationship, we developed a mouse model of $K_{ir}3.4$ autoimmunity. Electrophysiological study in $K_{ir}3.4$-immunized mice showed that $K_{ir}3.4$ autoantibodies significantly reduced atrial effective refractory period and predisposed animals to a 2.8-fold increased susceptibility to AF.

CONCLUSIONS: To our knowledge, this is the first report of an autoimmune pathogenesis of AF with direct evidence of $K_{ir}3.4$ autoantibody-mediated AF.

Key Words: atrial fibrillation ■ autoantibody ■ autoimmunity ■ I_{KACh} ■ $K_{ir}3.4$

Editorial, see p XXX

Atrial fibrillation (AF) is an ever-growing pandemic, with >46.3 million affected individuals worldwide.[1] Thromboembolism and heart failure are the major complications, associated with increased mortality.[1] Cardiovascular risk factors (eg, obesity, arterial hypertension, and diabetes) contribute to the development of AF, whereas structural heart diseases and valvulopathies represent common underlying causes.[1] Nevertheless, it is estimated that an underlying pathogenesis cannot be found in at least 3% of patients with AF.[2,3] Contrary to past assumptions, emerging evidence portends the involvement of autoantibodies in cardiac arrhythmias.[4–6] Because cardiac ion channels are key regulators of the heart rhythm, any perturbance of their function disrupts cardiac electrophysiology and can eventually trigger arrhythmias. Anti-Ro/SSa IgG is an archetypal autoantibody leading to cardiac conduction diseases, whereas autoantibodies binding to calcium and potassium channels (eg, $Ca_v1.2$, $K_v7.1$, and $K_v11.1$) have been implicated in ventricular arrhythmias.[4–6]

In the present study, we sought to identify an autoantibody signature of AF using high-throughput microarray

Correspondence to: Jin Li, MD, Department of Cardiology, University Heart Center, University Hospital Zurich, University of Zurich, Rämistrasse 100, 8091 Zurich, Switzerland; or Center for Translational and Experimental Cardiology, Department of Cardiology, University Hospital Zurich, University of Zurich, Wagistrasse 12, 8952 Schlieren, Switzerland. Email jin.li@usz.ch or jin.li@uzh.ch

Supplemental Material is available at https://www.ahajournals.org/doi/suppl/10.1161/CIRCULATIONAHA.120.047530.
For Sources of Funding and Disclosures, see page XXX.

Clinical Perspective

What Is New?

- This is the first study to systematically screen patients with atrial fibrillation (AF) for the presence of autoantibodies targeting cardiac ion channels.
- $K_{ir}3.4$ autoantibodies are detected in patients with unexplained AF.
- $K_{ir}3.4$ autoantibodies increase I_{KACh} current to shorten atrial repolarization and induce AF.

What Are the Clinical Implications?

- The present study introduces a novel form of autoimmune AF, caused by $K_{ir}3.4$ autoantibodies.
- The diagnosis of an autoimmune AF suggests that affected patients may benefit from a fundamentally different treatment approach than traditional AF.

Nonstandard Abbreviations and Acronyms

AERP	atrial effective refractory period
AF	atrial fibrillation
APD	action potential duration
Ca_v	voltage-gated calcium channel
d	end-diastole
hiPSC-aCMC	human induced pluripotent stem cell–derived atrial cardiomyocyte
$I_{Ca,L}$	L-type calcium current
I_{KACh}	acetylcholine-activated inwardly rectifying potassium current
I_{Kur}	ultrarapid delayed rectifier potassium current
I_{K1}	inward rectifier potassium current
I_{Na}	sodium current
I_{to}	transient outward potassium current
K_{ir}	inwardly rectifying potassium channel
K_v	voltage-gated potassium channel
LV	left ventricular
LVID	left ventricular internal diameter
MiRP	MinK-related peptide
pre-AF	incident atrial fibrillation during follow-up
s	end-systole

technology. We then performed patch clamp experiments to assess the electrophysiological properties of detected autoantibodies on atrial cardiomyocytes. Finally, we validated the arrhythmogenicity of detected autoantibodies in an experimental mouse model of immunization.

METHODS

The data, analytical methods, and study materials are made available to other researchers for purposes of reproducing the results and replicating the procedure. All data that support the findings of this study are made publicly available at the ZENODO repository and can be accessed at doi: 10.5281/zenodo.7491428.

Patient Samples

The study was conducted in accordance with the Declaration of Helsinki and the guidelines of Good Clinical Practice issued by the International Conference on Harmonization. Institutional review board approval and informed consent by the patient were obtained. Plasma samples used in this study were collected from patients diagnosed with unexplained AF (either pre-existent, referred to as AF, or incident during follow-up, referred to as pre-AF) and age-/sex-matched healthy individuals (referred to as controls). Unexplained AF was defined as AF in the absence of a direct underlying cause, in terms of secondary AF, such as structural heart disease, valvulopathies, or thyroid dysfunction.[3] Modifiable cardiovascular risk factors (eg, arterial hypertension, diabetes, dyslipidemia, and obesity) were not considered criteria of exclusion to obtain data from subjects, representative of real-world populations, in which these factors often coexist. Detailed Methods are provided in the Supplemental Material.

Peptide Microarray Assay

Peptides corresponding to extracellular sequences of all cardiac ion channels were translated into PEPperCHIP Custom Peptide Microarrays (PEPperPRINT GmbH, Heidelberg, Germany), as previously described.[7] Because anti–M_2-muscarinic acetylcholine and anti–β_1-adrenergic receptor autoantibodies have been associated with AF, both peptide sequences were included in the microarray assays.[4–6,8,9] Briefly, all plasma samples were diluted 1:30, followed by incubation with secondary (goat antihuman IgG [Fc] DyLight680) and control antibody (mouse monoclonal antihemagglutinin [12CA5] to confirm assay quality and the peptide microarray integrity). The LI-COR Odyssey Imaging System was used for scanning and readout. Microarray images were analyzed with the PepSlide Analyzer, as detailed previously.[7]

IgG Purification

Anti-$K_{ir}3.4$ autoantibodies were purified from pooled plasma of patients with AF with anti-$K_{ir}3.4$ IgG responses using affinity chromatography. The target $K_{ir}3.4$ peptide was immobilized through click chemistry through a C-terminal Lys(Azide) to dibenzocyclooctyne-functionalized column matrix (Peptide Specialty Laboratories GmbH, Heidelberg, Germany). Pooled plasma samples were diluted 1:1 with 1×PBS and applied onto the columns overnight at 4 °C with slow rotation. The total effluent was then run through the column twice. After several washing steps (3×1×PBS, 2×10 mmol/L Na-phosphate pH 6.8), the IgG antibodies were eluted from the column using Pierce IgG Elution Buffer (ThermoFisher Scientific, Zug, Switzerland) and collected in 2 mol/L K_2HPO_4. A diafiltration step was performed to transfer the purified IgGs into sterile 1×PBS pH 7.4.

The antibody concentrations were determined with a bicinchoninic acid assay (QuantiPro BCA Assay Kit, Sigma Aldrich GmbH, Buchs, Switzerland).

Human Induced Pluripotent Stem Cell–Derived Atrial Cardiomyocytes

Human induced pluripotent stem cell–derived cardiomyocytes with an atrial phenotype (hiPSC-aCMCs) were custom manufactured and provided by Ncardia BV (Leiden, The Netherlands). HiPSC-aCMCs were cultured according to manufacturer instructions, as previously described.[7,10] Further details on the atrial phenotype and handling of hiPSC-aCMCs are provided in the Supplemental Material. Pluricyte Cardiomyocyte Medium was changed every 48 hours until downstream patch clamp experiments (between days 7 and 12). Cells treated with anti-$K_{ir}3.4$ IgG (0.5 µg/mL) were preincubated for 24 hours before electrophysiological measurements.

Whole-Cell Patch Clamp Experiments

Patch clamp experiments were performed with EPC-10 amplifier controlled by PATCHMASTER (HEKA Elektronik GmbH, Lambrecht, Germany) to record cardiac action potentials and the acetylcholine-regulated inward rectifier K^+ current, I_{KACh}.[7,10] All measurements were performed at 37 °C. In brief, to record action potentials on spontaneously beating cardiomyocytes under current clamp conditions, the following external (Tyrode) solution was used (mmol/L): 140 NaCl, 5 KCl, 1 $MgCl_2$, 10 HEPES, 1.8 $CaCl_2$, 10 glucose (pH 7.4 adjusted with NaOH)±anti-$K_{ir}3.4$ IgG (0.5 µg/mL). Filamented borosilicate glass pipettes (tip resistances 2–4 MOhm, Harvard Apparatus, Holliston, MA) were filled with (mmol/L) 110 K^+aspartate, 20 KCl, 1 $MgCl_2$, 5 Mg^{2+}ATP, 0.1 Li^+GTP, 10 HEPES, 5 Na^+phosphocreatine, 0.05 EGTA (pH 7.3 adjusted with KOH), and 200 µg/mL amphotericin B. To record I_{KACh}, 10 µmol/L nifedipine (to inhibit the L-type Ca^{2+} current, I_{CaL}), 2 mmol/L 4-aminopyridine (to suppress the ultrarapid outward current, I_{Kur}, and the transient outward current, I_{to}), and 10 µmol/L ML-133 (Alomone Labs, Jerusalem, Israel, to block the background inward rectifier current, I_{K1}) were added to the Tyrode external solution±anti-$K_{ir}3.4$ IgG (0.5 µg/mL). Of note, Tertiapin Q, a selective inhibitor of I_{KACh}, has been traditionally used in patch clamp studies to record I_{KACh} current after a digital subtraction step of I_{K1} out of the inward rectifier K^+ current. Because Tertiapin Q binds to the extracellular pore loop domain of $K_{ir}3.4$, its presence would have interfered with anti-$K_{ir}3.4$ IgG and vice versa.[11–13] Both share the same extracellular target site, so the coadministration would potentially result in binding competition (eg, through steric hindrance). To circumvent this issue, we therefore applied ML-133, a novel selective I_{K1} inhibitor, to directly record I_{KACh}.[14] Borosilicate glass capillaries with tip resistances of 5 to 7 MOhm were filled with internal solution composed of (mmol/L) 110 K^+aspartate, 20 KCl, 1 $MgCl_2$, 5 Mg^{2+}ATP, 0.1 Li^+GTP, 10 HEPES, 5 Na^+phosphocreatine, and 5 EGTA (pH 7.3 adjusted with KOH). To stimulate I_{KACh}, the nonselective agonist carbachol, 10 µmol/L, was applied. For each set of experiments, measurements were collected between 10 and 120 minutes. The liquid junction potential was compensated (12.4 mV). The action potential duration (APD) at 90% repolarization, maximum diastolic potential, action potential amplitude, and beating rates were determined with FITMASTER (HEKA Elektronik GmbH, Lambrecht, Germany). I_{KACh} currents were elicited with a holding potential of −40 mV (to prevent the activation of the sodium current, I_{Na}), followed by 4-s test pulses between −120 mV and −20 mV in 10 mV-incremental steps. I_{KACh} currents were expressed as densities (pA/pF) to normalize for cell size. I_{KACh} data were analyzed with FITMASTER.

Study Animals and Design

Experiments were performed on Balb/c mice (8 weeks of age at first immunization; Charles River, France). Male and female mice were used in equal proportions. Immunization was carried out by BIOTEM (Apprieu, France) in accordance with a previously described protocol.[15–17] The peptide (IETETTIGYGFRVITEKPEC) was synthesized by BIOTEM (Apprieu, France). Of note, the target amino acid sequence is highly conserved between human and murine $K_{ir}3.4$ protein. Because the peptide contains an internal cysteine, a protected cysteine (C) was added during synthesis (IETETTIGYGFRVITEK(C)PEC) and deprotected after coupling to the carrier protein KLH. Mice from the $K_{ir}3.4$-immunized group received a subcutaneous injection of 100 µg of peptide supplemented with Complete Freund Adjuvant (day 0), followed by weekly injections of 50 µg of peptide and Incomplete Freund Adjuvant on days 7, 14, and 21. Mice from the control group were subjected to sham immunization (ie, Complete Freund Adjuvant and Incomplete Freund Adjuvant injections without peptide). ELISA was performed to quantify the IgG antibody titers on day 28 (Supplemental Material). All animals then underwent an echocardiographic assessment of their cardiac function as well as in vivo electrophysiological study. All animal procedures followed the guidelines of the Ethics Committee for Animal Experimentation of the Swiss Academy of Medical Sciences and the Swiss Academy of Sciences (BE97/2021).

Transthoracic Echocardiography

Echocardiograms were obtained using a 15L8-S transducer (15-8MHz) connected to the Acuson Sequoia C512 system (Siemens Healthcare AG, Switzerland) with the echocardiographer blinded to the group allocation of the animals. All mice were anesthetized with isoflurane (3.5% for induction and 1.5%–2% for maintenance) mixed with 2 L/min oxygen. Core temperature was maintained at 37 °C. Left ventricular internal diameter (LVID), anterior and posterior left ventricular (LV) wall thickness, both at end-diastole (d) and end-systole (s), were measured using the M-mode in short-axis view, at the level of the papillary muscle. LV fractional shortening was calculated as fractional shortening (%)=100×[(LVIDd–LVIDs/LVIDd], whereas LV ejection fraction was calculated as ejection fraction (%)=100×[(LVIDd^3-LVIDs^3)/LVIDd^3].[18] Left atrial diameter was obtained with B-mode in the parasternal long-axis view.

Electrocardiography and Electrophysiological Study

Anesthesia was induced with 3.5% isoflurane and maintained at 1.5% to 2% isoflurane with 2 L/min oxygen flow rate. The body temperature was kept at 37 °C with a heating pad, and

all mice were continuously monitored with surface 3-lead ECG connected to the data acquisition system PowerLab (16/35, ADInstruments Ltd, United Kingdom). 29-Gauge needle electrodes were placed at the base of the limbs. Baseline ECG intervals (RR, PR, QRS, QT, and JT) were calculated in lead I or II for each animal, on the basis of averages of 10 consecutive complexes. The formula proposed by Mitchell et al was used for heart rate correction of the QT and JT intervals: $QTc = QT/(RR/100)^{1/2}$ and $JTc = JT/(RR/100)^{1/2}$, respectively.[19,20] A 1.1F octapolar electrophysiology catheter (ADInstruments Ltd, United Kingdom) was inserted into the right internal jugular vein to record intracardiac electrograms. Bipolar electrogram recordings were obtained from the right atrium and the right ventricle (sampling rate 4 k/s, filtered between 0.5 and 500 Hz). Stimulation was performed with 2-ms pulse width at twice the diastolic threshold. Standard electrophysiological pacing protocols were adopted to measure basic parameters.[18,21,22] To evaluate the sinus node function, the right atrium was paced at 100 ms during 15 s. Sinus node recovery time was defined as the time interval between the last stimulus of pacing train and the onset of first spontaneous atrial signal. Corrected sinus node recovery time was calculated as the difference between sinus node recovery time and the sinus cycle length before stimulation. We determined the atrioventricular conduction properties with rapid atrial pacing of 2-s durations, starting at a basic cycle length of 100 ms and decrements of 10-ms intervals. The anterograde Wenckebach cycle length was defined as the pacing rate at which the loss of 1:1 atrioventricular conduction occurs. To assess effective refractory periods of the atrium and the atrioventricular node (AERP and atrioventricular effective refractory period, respectively), the atrium was stimulated with a train of 9 stimuli at a fixed pacing cycle length (S1) of 100 ms followed by an extrastimulus (S2) introduced at progressively shorter coupling intervals. The stepwise reduction in S1-S2 interval by 2-ms decrements started at 70 ms until S2 no longer conducted to the ventricles through the atrioventricular node (atrioventricular effective refractory period) and until S2 no longer induced an atrial signal (AERP; minimum coupling interval of 20 ms). Inducibility of AF was tested by using standard burst pacing protocols, as previously described.[18,21–23] Briefly, 2-s bursts with decremental cycle lengths of 40 ms to 20 ms (in 2-ms steps) were applied. Next, atrial burst pacing was performed with 300 cycles of 2-ms bursts and a cycle length of 50 ms, 40 ms, 30 ms, 20 ms, and 10 ms. AF was defined as lack of regular P-waves and irregularly irregular QRS complexes on ECG, in combination with rapid, fragmented atrial electrograms with irregular ventricular rhythm, lasting at least 2 s. If 1 or more bursts in either protocol evoked an AF episode, AF was considered to be inducible in that animal. The investigator performing and analyzing the electrophysiological study was blinded to the group assignment of the mice. All data were analyzed using LabChart 8 software (ADInstruments Ltd, United Kingdom).

Statistical Analysis

The statistical analysis of microarrays was based on the background-corrected median intensities of IgG responses against a hundred different peptides. Data analysis was performed with R language (R version 4.0.2). A positive response was defined as ≥100 fluorescence intensity units, and signals <100 fluorescence intensity units were set as 0, accordingly. Peptides with 0 fluorescence intensity units in all individuals were removed, and the remaining 84 peptides were used for statistical analysis. The remaining raw values of IgG of the 84 peptides were normalized using variance stabilizing normalization.[24] The variance stabilizing normalized data were used for 1-way ANOVA to identify differential IgG responses in AF and pre-AF versus control, respectively. We defined false discovery rate adjusted *P* values of <-0.10 as threshold for statistical significance of an IgG response, using the Benjamini-Hochberg correction method. In addition, a principal component analysis was performed with the microarray data to visualize pattern between samples and identify clustering in patients with AF according to IgG profiles.

Electrophysiological in vitro and in vivo data were tested for normality with the Shapiro-Wilk test. Normally distributed patch clamp data of similar variance were compared by 1-way ANOVA, followed by Tukey post hoc test. The Kruskal-Wallis test was used when the normality assumption was not met with the Dunn multiple-comparisons test. Because data derived from the murine model (echocardiography, ECG, and electrophysiological study) compared sham- with $K_{ir}3.4$-immunized mice, parametric data were analyzed with the Student *t* test, whereas nonparametric parameters were compared with the Mann-Whitney *U* test. Categorical variables (AF inducibility) were compared using the Fisher exact test. Statistical analyses were performed with GraphPad Prism 9 (GraphPad Software, Inc, La Jolla, CA). A *P* value < 0.05 was considered statistically significant.

RESULTS

Study Population

Thirty-seven patients diagnosed with unexplained AF were age- and sex-matched with 37 healthy controls (Table S1). The patient demographics included 34 female and 40 male participants, with a mean age of 69.8±16.4 years. Another 14 patients (pre-AF) had no documented AF at baseline but developed unexplained AF during a mean follow-up of 52 months. Before the diagnosis of AF, patients were in the same age range (67.5±7.5 years) as the cohort with established AF (*P*=0.822; Table S1).

Autoantibody Signature of AF

A tailored peptide microarray was used to map the IgG responses to cardiac ion channels in patients with and without AF (Table S2). Figure 1 illustrates the analysis workflow. In general, we observed autoantibody responses in all 3 groups, with higher reactivities in patients with AF compared with pre-AF and healthy subjects. The principal component analysis did not show any particular clustering of AF and pre-AF samples (Figure S1). The results of 1-way ANOVA were sorted by decreasing mean differences and summarized in Table 1. We found statistically significant autoantibodies reacting with the IETETTIGYGFRVITEKCPE ($K_{ir}3.4$ protein) and

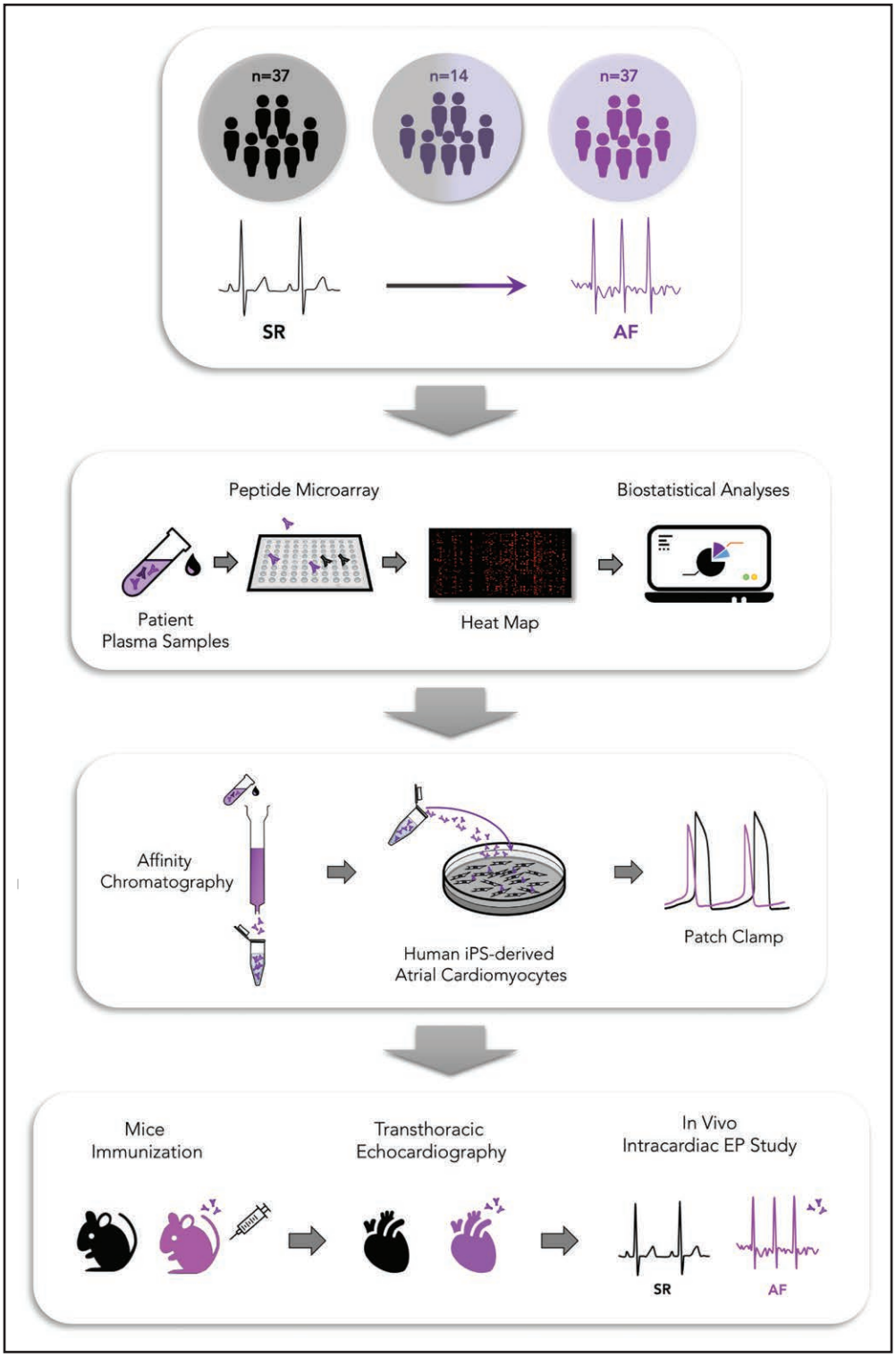

Figure 1. Overview of analysis workflow.
Diagram showing the analysis workflow of the present study: 37 patients with AF, 37 age- and sex-matched healthy controls, and 14 patients before the development of AF (pre-AF) were enrolled. Using peptide microarray, plasma samples were screened for the presence of autoantibodies targeting a panel of cardiac ion channels. The heat map of peptides was analyzed for immunoreactivity across all plasma samples. The identified autoantibody was then purified using affinity chromatography and tested on human atrial cardiomyocytes. Mice immunized with the target peptide produced autoantibodies to replicate the human condition. No structural heart abnormalities were evident, and electrophysiological in vivo study confirmed an increased AF susceptibility in immunized mice. AF indicates atrial fibrillation; EP, electrophysiological; iPS, induced pluripotent stem cell; and SR, sinus rhythm.

Table 1. AF-Specific Autoantibody Reactivities in Plasma Samples

Peptide	Protein	Mean Pre/AF	Mean control	Mean difference	Unadjusted *P* value	FDR-adjusted *P* value
AF vs control						
IETETTIGYGFRVITEKCPE	$K_{ir}3.4$	1.027	0.000	1.027	0.0136	0.0299
SNFTQTLEDVFRRIFITYMD	MiRP	0.980	0.149	0.831	0.0450	0.0676
LMVTMSTVGYGDVYAKTTLG	BK_{Ca}	0.000	1.137	−1.137	0.0237	0.0712
Pre-AF vs control						
IETETTIGYGFRVITEKCPE	$K_{ir}3.4$	2.382	0.000	2.382	0.0199	0.0299
LCIGYGRQAPVGMSDVWLTM	HCN4	0.000	0.562	−0.562	0.0841	0.0841
SIHSFSSAFLFSIEVQVTIG	$K_{ir}6.2$	0.000	0.995	−0.995	0.0239	0.0359
LFKGKLYTCSDSSKQTEAEC	$Ca_v1.2$	0.000	1.618	−1.618	0.0017	0.0051

Represented are the peptides that demonstrated the highest IgG response in the control, AF, and pre-AF groups. The ranking was based on differences reflecting the overall intensity ratio between groups. Using ANOVA, the mean IgG responses were compared between control, AF, and pre-AF. AF indicates atrial fibrillation; FDR, false discovery rate correction for AF vs control and pre-AF vs control; and MiRP, MinK-related peptide.

SNFTQTLEDVFRRIFITYMD (MiRP protein [MinK-related peptide]) peptides in patients with AF, whereas anti-LMVTMSTVGYGDVYAKTTLG (large-conductance calcium-activated potassium channel protein) IgG predominated in healthy controls. Of patients with AF, 16.2% presented anti-$K_{ir}3.4$ autoantibodies compared with none in healthy controls. Next, we screened patients with no AF at baseline, but incident AF during follow-up. High IgG reactivities to the identical peptide sequence of the $K_{ir}3.4$ protein (IETETTIGYGFRVITEKCPE) were detected in 35.7% of pre-AF samples. Table S3 lists the clinical characteristics and anti-$K_{ir}3.4$ autoantibody status for each patient.

$K_{ir}3.4$ Autoantibody

To assess the role of $K_{ir}3.4$ autoantibodies, we first purified the IgG out of plasma samples of patients with AF. We then tested the response of hiPSC-aCMCs to muscarinic cholinergic stimulation. The application of the agonist, 10 µmol/L carbachol, resulted in APD shortening by 21% (mean APD at 90% repolarization in control cells, 390.2±50.5 ms versus carbachol, 307.2±24.0 ms; *P*=0.157; Figure 2A and 2B; Table S4), thus confirming the presence of M_2-muscarinic receptors and $K_{ir}3.1/3.4$ channels, which is in agreement with the literature.[25–27] For I_{KACh} current recordings, the selective $K_{ir}2$ channel blocker, ML-133, was used to discriminate between the inward rectifying K^+ currents' contributions, I_{K1} and I_{KACh}.[14] A reversal potential around the equilibrium potential for K^+ was measured (−80 mV; Figure 2D). As expected, carbachol increased I_{KACh} current (at −120 mV, mean I_{KACh} in control cells, −6.9±2.3 pA/pF, versus carbachol, −11.8±1.2 pA/pF; *P*=0.040), thereby confirming the atrial phenotype of the cardiomyocytes. Figure 2 shows typical action potentials and I_{KACh} currents recorded in cells under control conditions and in response to muscarinic cholinergic stimulation. Next, we applied $K_{ir}3.4$ autoantibodies extracted from patients with AF. Anti-$K_{ir}3.4$ IgG shortened the APD by one-third (mean APD at 90% repolarization in control cells, 390.2±50.5 ms versus anti-$K_{ir}3.4$ IgG, 261.5±17.5 ms; *P*=0.012; Figure 2A and 2B) and led to a 2-fold increase in I_{KACh} current (mean I_{KACh} at −120 mV in control cells, −6.9±2.3 pA/pF, versus anti-$K_{ir}3.4$ IgG, −13.7±1.1 pA/pF; *P*=0.003; Figure 2C and 2D). The addition of carbachol did not further potentiate the effect of anti-$K_{ir}3.4$ IgG (*P*>0.05 when comparing anti-$K_{ir}3.4$ IgG and anti-$K_{ir}3.4$ IgG + carbachol). The mean cell capacitance did not differ between groups (*P*=0.970): control cells, 40.5±13.0 pF; with carbachol, 48.5±14.2 pF; with anti-$K_{ir}3.4$ IgG, 35.8±5.1 pF; with anti-$K_{ir}3.4$ IgG and carbachol, 62.6±25.8 pF. Table S4 summarizes the parameters of action potentials for each set of experiments.

$K_{ir}3.4$ Autoimmunity

Next, we developed an experimental mouse model of immunization to validate the arrhythmogenic role of $K_{ir}3.4$ autoantibodies in vivo (Figure 3A). After $K_{ir}3.4$ immunization, all mice generated $K_{ir}3.4$ autoantibodies (anti-$K_{ir}3.4$ IgG titers >1:3000). Sham-immunized mice served as controls and accordingly presented no detectable titers. Two $K_{ir}3.4$-immunized mice died 1 week after full immunization and before completion of cardiac examinations. No previous progressive deterioration was observed. Nevertheless, the cause of death remains unknown. In general, all mice exhibited no signs of heart failure, such as edema or dyspnea. Body and heart weights were similar between groups (Table 2). $K_{ir}3.4$ autoantibodies had no effect on cardiac structure or function (Table 2). All mice showed a preserved LV ejection fraction and normal left atrial dimensions on echocardiography (Table 2). Representative ECG traces are depicted in Figure 3B. All mice presented a normal sinus rhythm, and no differences in ECG intervals were found between groups (Figure 3B and 3C,;Table S5). During intracardiac electrophysiological study, we recorded no changes in sinus and atrioventricular nodal function in the presence of $K_{ir}3.4$ autoantibodies (Figure 3; Table S5). However, we measured a significantly shorter AERP in mice with $K_{ir}3.4$ autoantibodies compared with

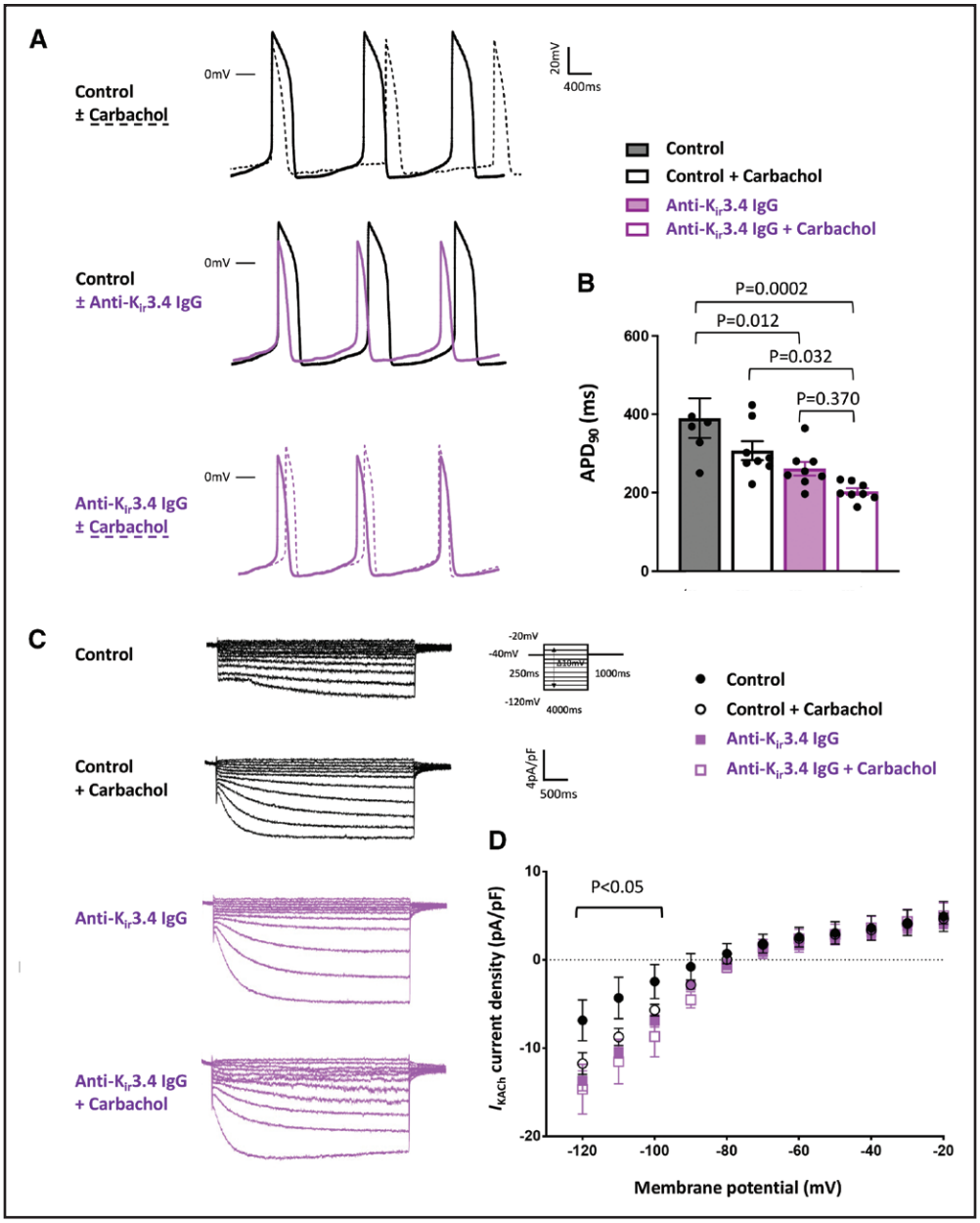

Figure 2. Cardiac action potentials and I_{KACh} current recorded in human induced pluripotent stem cell–derived atrial cardiomyocytes (hiPSC-aCMCs).

A, Representative action potential traces recorded in hiPSC-CMCs under control condition, in response to 10 μmol/L carbachol and ±0.5 μg/mL anti-K_{ir}3.4 IgG. **B,** Mean action potential duration±SEM determined at 90% repolarization (APD_{90}) obtained in control cells (390.2±50.5 ms; n=6), in response to 10 μmol/L carbachol (307.2±24.0 ms; n=8), in the presence of 0.5 μg/mL anti-K_{ir}3.4 IgG (261.5±17.5 ms; n=8) vs 0.5 μg/mL anti-K_{ir}3.4 IgG in addition to 10 μmol/L carbachol (203.2±8.3 ms; n=8). Statistical significance was determined using 1-way ANOVA with Tukey multiple comparisons test. **C,** Representative I_{KACh} currents normalized to cell capacitance recorded in control cells, in response to 10 μmol/L carbachol, in the presence of 0.5 μg/mL anti-K_{ir}3.4 IgG with and without the addition of 10 μmol/L carbachol. The voltage step stimulation protocol is outlined. **D,** Mean current density-voltage relationships (±SEM) of cells under control condition (n=4), in response to 10 μmol/L carbachol (n=7), in the presence of 0.5 μg/mL anti-K_{ir}3.4 IgG with (n=5) and without the addition of 10 μmol/L carbachol (n=6). To record I_{KACh}, 10 μmol/L nifedipine ($I_{Ca,L}$ inhibition), 2 mmol/L 4-aminopyridine (I_{Kur} and I_{to} inhibition), and 10 μmol/L ML-133 (I_{K1} inhibition) were added to the external solution. All data were measured at 37 °C. Statistical significance was determined using Kruskal-Wallis followed by Dunn multiple-comparisons test.

control animals (*P*=0.0012; Figure 3E; Table S5). Because reduced AERP promotes multiple-circuit reentry in the atrial tissue, we next examined the susceptibility of each mouse to develop AF on rapid atrial pacing. Using standard burst pacing protocols, AF was inducible in 80% (8 of 10) of mice with K_{ir}3.4 autoantibodies compared with 28% (4 of 14) in seronegative mice (*P*=0.0361; Figure 3D and 3F). Previous works have induced similar

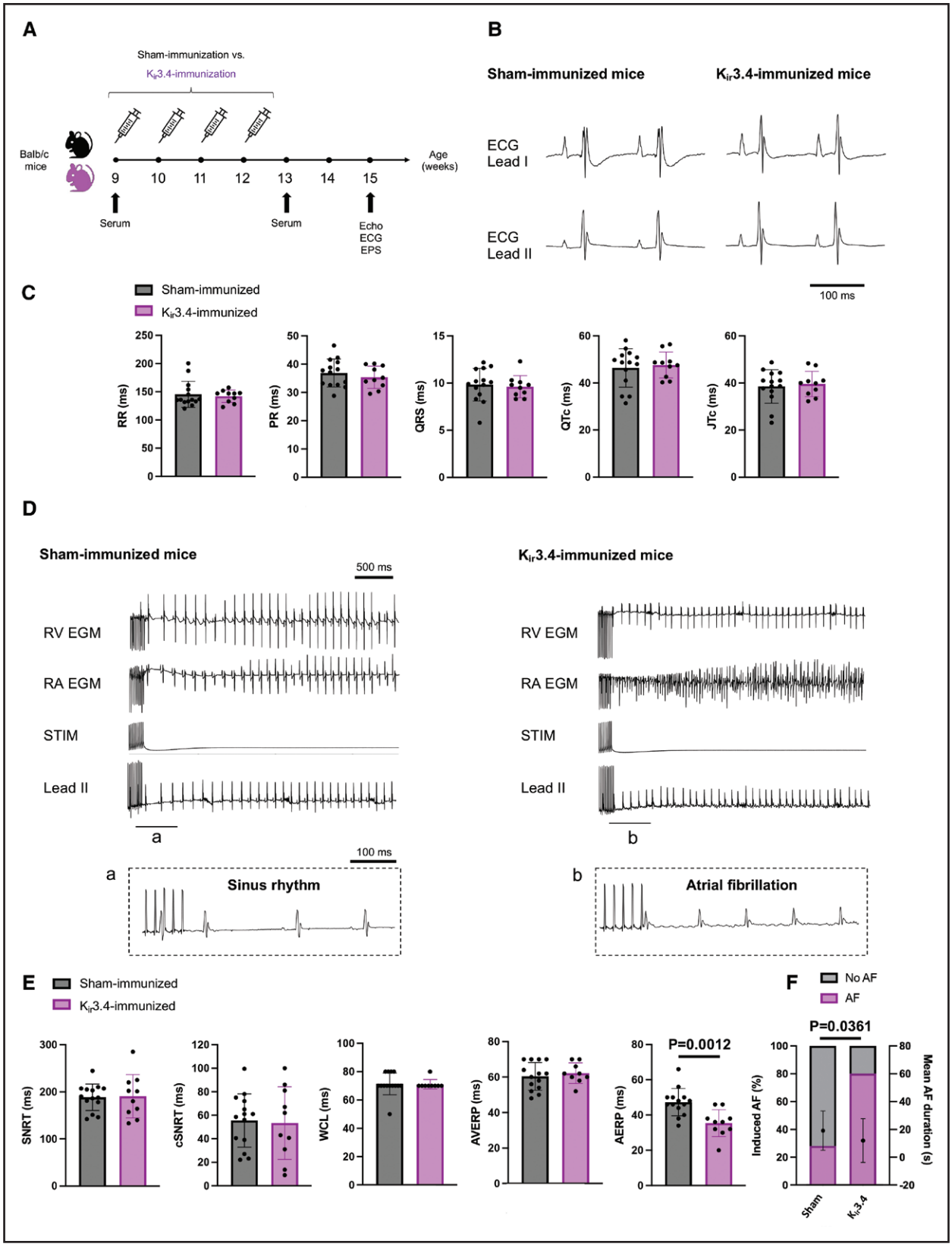

Figure 3. Electrophysiological phenotyping of mice with K_{ir}3.4 autoantibodies.
A, Study design of the experimental autoimmune AF model with Balb/c mice. **B,** Representative surface ECG traces derived from limb leads I and II, recorded from a sham-immunized and K_{ir}3.4-immunized mouse. **C,** Bar graphs overlaid with dot plots present mean ECG interval values±SD recorded in sham- (n=14) and K_{ir}3.4-immunized mice (n=10). Statistical significance was determined using the Student *t* test (PR, QRS, QTc, and JTc) and Mann-Whitney *U* test (RR). **D,** Representative bipolar intracardiac electrogram recordings at the level of the right ventricle (*Continued*)

Figure 3 Continued. (RV) and right atrium (RA). STIM denotes right atrial stimulation. ECG in lead II configuration shows the corresponding surface ECG signals. **E,** Bar graphs overlaid with dot plots present mean intracardiac electrophysiological data±SD acquired in sham- (n=14) and K_{ir}3.4-immunized mice (n=10). Statistical significance was determined using the Student *t* test (SNRT, cSNRT, AERP, and AVERP) and Mann-Whitney *U* test (WCL). **F,** Bar graph shows the proportion of sham- (4 of 14) and K_{ir}3.4-immunized mice (8 of 10) with burst pacing–induced AF. Points indicate mean AF duration±SD (*P*=0.214). Statistical significance was determined by Mann-Whitney *U* test (AF duration), and Fisher exact test was used to assess the induced AF rate. AERP indicates atrial effective refractory period; AF, atrial fibrillation; AVERP, atrioventricular effective refractory period; cSNRT, corrected sinus node recovery time; EGM, electrogram; EPS, electrophysiological study; RR, relative risk; SNRT, sinus node recovery time; and WCL, Wenckebach cycle length.

rates of AF in control mice and on cholinergic activation with carbachol.[28–31] Collectively, K_{ir}3.4 autoantibodies contribute to a 2.8-fold increased vulnerability to AF (relative risk, 2.8 [95% CI, 1.2–7.1]).

DISCUSSION

In the present study, we used a peptide microarray displaying the cardiac ion channel repertoire to establish the autoantibody profile of patients with AF. One single autoantibody targeting the extracellular site of the K_{ir}3.4 protein (IETETTIGYGFRVITEKCPE peptide sequence; Figure S2) consistently discerned patients with AF from controls. Intriguingly, patients with pre-existent and incident AF during follow-up had in common the presence of K_{ir}3.4 autoantibodies. In an effort to explore further a potential link between K_{ir}3.4 autoantibodies and AF, we undertook cellular and animal studies. We first described K_{ir}3.4 autoantibody-induced reduction in atrial refractoriness, resulting in increased AF susceptibility.

In the past, studies have associated autoantibodies against myosin heavy chain, heat shock proteins, M_2-muscarinic acetylcholine, and β_1-adrenergic receptors with AF.[4–6,8,9] Whereas anti–myosin heavy chain and anti–heat shock protein IgG have in fact been associated with AF but with no clear causal link, autoantibodies targeting the G protein–coupled receptors have essentially been the focus of autoimmune AF research.[4–6] The autonomic nervous system initiates a sequence of signaling effects contributing to atrial structural and electrophysiological remodeling prone to AF.[32,33] Nevertheless, in the present study, we also screened patients for the presence of anti–M_2-muscarinic and anti–β_1-adrenergic receptor autoantibodies but failed to detect any significant IgG reactivities to said receptors.

To the best of our knowledge, this is the first study to describe the existence of autoantibodies targeting a cardiac ion channel subunit, K_{ir}3.4, in AF. The K_{ir}3.4 target protein is of particular interest, given its atrial-selective expression.[34] In the heart, K_{ir}3.4 forms a functional heterotetramer with the K_{ir}3.1 subunit that underlies the acetylcholine-gated K_{ACh} channel (formerly known as GIRK1/GIRK4 [G protein–activated inwardly rectifying K^+ channel]). The notion of altered inward rectifier K^+ currents in AF was first described >20 years ago.[35] Although initial observations accounted I_{K1} for AF, subsequent studies have pointed to the importance of I_{KACh} current in the pathogenesis of AF.[33,36–39] The I_{KACh} pathway essentially mediates the negative chronotropic effect of the parasympathetic nervous system. The resulting shortened atrial APD, reduced AERP, and enhanced dispersion of atrial repolarization provide an arrhythmogenic substrate for AF.[33,38–40] I_{KACh} has 2 components, namely an acetylcholine-regulated and a constitutively active (agonist-independent) form. A sustained high atrial rate (atrial tachycardia) was found to increase the open probability of constitutively active I_{KACh} channels that eluded the muscarinic cholinergic regulation.[38,39] Together with Ca^{2+} handling abnormalities, atrial contractility and conduction are impaired, giving way to reentry circuits and AF maintenance.[33] Here, we discovered in patients with AF a K_{ir}3.4 autoantibody that increased I_{KACh}, in the absence of muscarinic cholinergic stimulation. This is the first report of an autoantibody-induced constitutive I_{KACh} current.

Table 2. Weight Parameters and Echocardiographic Data

	Sham-immunized mice (n=14)	K_{ir}3.4-Immunized mice (n=10)	*P* value
Weight parameters			
BW, mean±SD, g	27.3±2.5	27.7±2.2	0.705
HW, mean±SD, mg	147.9±32.6	134.6±11.8	0.250
HW/TL, mean±SD, mg/mm	8.3±1.7	7.4±0.6	0.137
Echocardiography			
LA, mean±SD, mm	2.3±0.2	2.3±0.2	0.989
AWd, mean±SD, mm	1.2 ±0.2	1.2±0.1	0.943
LVIDd, mean±SD, mm	3.4±0.4	3.1±0.4	0.198
PWd, mean±SD, mm	1.3±0.3	1.3±0.2	0.817
AWs, mean±SD, mm	1.7±0.2	1.6±0.2	0.097
LVIDs, mean±SD, mm	2.0±0.5	1.9±0.5	0.465
PWs, mean±SD, mm	1.6±0.3	1.6±0.3	0.853
FS, mean±SD, %	51.1±9.0	49.8±8.1	0.719
EF, mean±SD, %	76.7±11.6	78.7±11.9	0.676

Statistical significance was determined using the Student *t* test (BW, LA, LVIDd, PWd, AWs, LVIDs, PWs, FS, and EF) and Mann-Whitney *U* test (HW, TL, HW/TL, and AWd).

AWd indicates end-diastolic anterior wall thickness; AWs, end-systolic anterior wall thickness; BW, body weight; EF, ejection fraction; FS, fractional shortening; HW, heart weight; LA, left atria; LVIDd, end-diastolic left ventricular internal diameter; LVIDs, end-systolic left ventricular internal diameter; PWd, end-diastolic posterior wall thickness; PWs, end-systolic posterior wall thickness; and TL, tibia length.

This has prompted us to validate the findings in an experimental autoimmune model, in which mice were immunized to generate autoantibodies targeting I_{KACh} channels. In the same way that increased parasympathetic tone promotes AF, $K_{ir}3.4$ autoantibodies in mice reduced atrial refractoriness, thus giving way to reentry wavelets and AF.[28–31,41,42] The pathogenesis of AF is complex and essentially requires 2 critical components: a trigger that initiates the event and a substrate that maintains the arrhythmia.[33] Consistent with this notion, we detected $K_{ir}3.4$ autoantibodies in patients with no structural heart disease before AF manifests clinically. The absence of AF at baseline in these patients despite the presence of $K_{ir}3.4$ autoantibodies may mean that a structural (eg, fibrosis or inflammation) or electrical substrate (tissue anisotropy secondary to heterogeneous atrial deposition of IgG) is required in addition to the I_{KACh} trigger to initiate AF. Future large cohorts will be important to determine the prevalence of autoimmune AF. In this sense, $K_{ir}3.4$ autoantibody, as an independent AF risk factor, would present a powerful predictive blood biomarker for patients.

One limitation of the present study is that systematic prolonged ECG monitoring was not performed, raising the possibility that patients with AF but without clinical symptomatology were not accounted for in the analysis. We did not profile serially autoantibodies in any given patient and did not differentiate between AF types (paroxysmal, persistent, long-standing persistent, and permanent). We opted for a more lenient definition of unexplained AF rather than stringent (excluding patients with modifiable risk factors), given that a link between autoantibodies and cardiovascular risk factors has been established, and both conditions may coexist.[43–45] Excluding patients with cardiovascular risk factors from our autoantibody screening would therefore have potentially introduced a selection bias. Moreover, microvesicles shed from cardiomyocytes after mechanical stress (cardiovascular risk factors) may release cell-specific proteins embedded in lipid bilayers into the systemic circulation and thus trigger an autoimmune response.[46–49] Little is known about ion channels and their topology in microvesicles originating from cardiomyocytes. Considering that the I_{KACh}-forming heterotetramer is composed of 2 $K_{ir}3.4$ and 2 $K_{ir}3.1$ subunits, we would have expected the concomitant detection anti-$K_{ir}3.1$ autoantibodies in patients with anti-$K_{ir}3.4$ autoantibodies.[50] On the basis of our peptide microarray assay, anti-$K_{ir}3.4$ autoantibodies were not accompanied by anti-$K_{ir}3.1$ autoantibodies (Pearson correlation coefficient, −0.04). In addition, microvesicles originating from atrial cardiomyocytes would also cover atrial-specific $K_v1.5$ channels, but no matching IgG responses were detected (Pearson correlation coefficients comparing $K_{ir}3.4$ and $K_v1.5$, −0.05 [RDERELLRHPPAPHQPPAPA], −0.04 [APPSGPTVAPLLPRTLADPF], and −0.07 [NQGTHFSSIPDAFWWAVVTM]). Altogether, the pathogenesis of circulating anti-$K_{ir}3.4$ autoantibodies remains to be elucidated in future investigations. In our study, 3 patients presented anti-$K_{ir}3.4$ autoantibodies in the absence of comorbidities. With that in mind, it is compelling to speculate that anti-$K_{ir}3.4$ autoantibodies could also present a source for reentry through activation of I_{KACh} channels expressed in pulmonary veins.[51] Furthermore, anti-$K_{ir}3.4$ autoantibodies in the present study were polyclonal in nature. Further studies are needed to investigate whether a monoclonal population may account for the initiation of AF. Although widely used and accepted, the mouse model is imperfect for the study of AF due to the insufficient critical mass of the structurally normal murine heart that prevents sustained reentry circuits.[29,30,52] For this reason, atrial pacing protocols have been introduced to use AF inducibility as a surrogate for human AF vulnerability. Likewise, we documented no spontaneous AF in $K_{ir}3.4$-immunized mice, but pacing-induced AF upon electrophysiological study.

Conclusions

We describe a novel, autoimmune form of AF that is caused by $K_{ir}3.4$ autoantibodies, thus adding a new pathogenic mechanism to the long list of causes of AF. Future studies will be needed to investigate the therapeutic benefit of removing arrhythmogenic $K_{ir}3.4$ autoantibodies from the circulation or of neutralizing antigen-binding sites of the antibody.[5,6,53]

ARTICLE INFORMATION

Received October 6, 2022; accepted June 1, 2023.

Affiliations

Institute of Physiology, University of Bern, Switzerland (A.M.). PEPperPRINT GmbH, Heidelberg, Germany (Y.M.). Montreal Heart Institute, Université de Montréal, Canada (J.-C.T., D.B.). Department of Cardiology, University Heart Center, University Hospital Zurich, University of Zurich, Switzerland (J.L.). Center for Translational and Experimental Cardiology, Department of Cardiology, University Hospital Zurich, University of Zurich, Schlieren,

Acknowledgments

The authors thank the excellent support provided by the team of PEPperPRINT GmbH, in particular, Sarah Schott. We are indebted to Sandra Caillet and Georgia Alaimo from BIOTEM for the outstanding collaboration on mice immunization. We thank Michael Känzig from the Institute of Physiology, University of Bern, for his invaluable technical assistance.

Sources of Funding

This work was supported by an Ambizione and an Eccellenza grant from the Swiss National Science Foundation (PZ00P3_173961 to J.L. and PCEFP3_203333 to J.L.).

Disclosures

Dr Tardif reports grants from Amarin; grants and personal fees from AstraZeneca; grants, personal fees, and minor equity interest from DalCor; personal fees from HLS Pharmaceuticals; grants from Ionis; grants from Pfizer; personal fees from Pendopharm; grants from RegenexBio; grants and personal fees from Sanofi; and personal fees from Servier, outside the submitted work. Dr Li reports previous employment by BioMarin Pharmaceutical Inc, outside the submitted work. Dr Maguy reports consultant fees from BioMarin Pharmaceutical Inc, outside the submitted work. The other authors report no conflicts.

Supplemental Material

Expanded Methods
Tables S1–S5
Figures S1–S2

REFERENCES

1. Hindricks G, Potpara T, Dagres N, Arbelo E, Bax JJ, Blomström-Lundqvist C, Boriani G, Castella M, Dan G-A, Dilaveris PE, et al; ESC Scientific Document Group. 2020 ESC guidelines for the diagnosis and management of atrial fibrillation developed in collaboration with the European Association for Cardio-Thoracic Surgery (EACTS): the Task Force for the diagnosis and management of atrial fibrillation of the European Society of Cardiology (ESC) developed with the special contribution of the European Heart Rhythm Association (EHRA) of the ESC. *Eur Heart J*. 2021;42:373–498. doi: 10.1093/eurheartj/ehaa612
2. Wyse DG, Van Gelder IC, Ellinor PT, Go AS, Kalman JM, Narayan SM, Nattel S, Schotten U, Rienstra M. Lone atrial fibrillation: does it exist? *J Am Coll Cardiol*. 2014;63:1715–1723. doi: 10.1016/j.jacc.2014.01.023
3. Roston TM, Islam S, Hawkins NM, Laksman ZW, Sanatani S, Krahn AD, Sandhu R, Kaul P. A population-based study of unexplained/lone atrial fibrillation: temporal trends, management, and outcomes. *CJC Open*. 2022;4:65–74. doi: 10.1016/j.cjco.2021.09.006
4. Lee H-C, Huang KTL, Wang X-L, Shen W-K. Autoantibodies and cardiac arrhythmias. *Heart Rhythm*. 2011;8:1788–1795. doi: 10.1016/j.hrthm.2011.06.032
5. Lazzerini PE, Capecchi PL, Laghi-Pasini F, Boutjdir M. Autoimmune channelopathies as a novel mechanism in cardiac arrhythmias. *Nat Rev Cardiol*. 2017;14:521–535. doi: 10.1038/nrcardio.2017.61
6. Li J. The role of autoantibodies in arrhythmogenesis. *Curr Cardiol Rep*. 2020;23:3. doi: 10.1007/s11886-020-01430-x
7. Maguy A, Tardif J-C, Busseuil D, Ribi C, Li J. Autoantibody signature in cardiac arrest. *Circulation*. 2020;141:1764–1774. doi: 10.1161/CIRCULATIONAHA.119.044408
8. Baba A, Yoshikawa T, Fukuda Y, Sugiyama T, Shimada M, Akaishi M, Tsuchimoto K, Ogawa S, Fu M. Autoantibodies against M2-muscarinic acetylcholine receptors: new upstream targets in atrial fibrillation in patients with dilated cardiomyopathy. *Eur Heart J*. 2004;25:1108–1115. doi: 10.1016/j.ehj.2004.05.012
9. Yalcin MU, Gurses KM, Kocyigit D, Kesikli SA, Ates AH, Evranos B, Yorgun H, Sahiner ML, Kaya EB, Oto MA, et al. Elevated M2-muscarinic and β1-adrenergic receptor autoantibody levels are associated with paroxysmal atrial fibrillation. *Clin Res Cardiol*. 2015;104:226–233. doi: 10.1007/s00392-014-0776-1
10. Maguy A, Kucera JP, Wepfer JP, Forest V, Charpentier F, Li J. KCNQ1 antibodies for immunotherapy of long QT syndrome type 2. *J Am Coll Cardiol*. 2020;75:2140–2152. doi: 10.1016/j.jacc.2020.02.067
11. Jin W, Lu Z. A novel high-affinity inhibitor for inward-rectifier K+ channels. *Biochemistry*. 1998;37:13291–13299. doi: 10.1021/bi981178p
12. Jin W, Klem AM, Lewis JH, Lu Z. Mechanisms of inward-rectifier K+ channel inhibition by tertiapin-Q. *Biochemistry*. 1999;38:14294–14301. doi: 10.1021/bi991206j
13. Yow TT, Pera E, Absalom N, Heblinski M, Johnston GAR, Hanrahan JR, Chebib M. Naringin directly activates inwardly rectifying potassium channels at an overlapping binding site to tertiapin-Q. *Br J Pharmacol*. 2011;163:1017–1033. doi: 10.1111/j.1476-5381.2011.01315.x
14. Wang H-R, Wu M, Yu H, Long S, Stevens A, Engers DW, Sackin H, Daniels JS, Dawson ES, Hopkins CR, et al. Selective inhibition of the K(ir)2 family of inward rectifier potassium channels by a small molecule probe: the discovery, SAR, and pharmacological characterization of ML133. *ACS Chem Biol*. 2011;6:845–856. doi: 10.1021/cb200146a
15. Kaya Z, Göser S, Buss SJ, Leuschner F, Ottl R, Li J, Völkers M, Zittrich S, Pfitzer G, Rose NR, et al. Identification of cardiac troponin I sequence motifs leading to heart failure by induction of myocardial inflammation and fibrosis. *Circulation*. 2008;118:2063–2072. doi: 10.1161/CIRCULATIONAHA.108.788711
16. Li J, Göser S, Leuschner F, Volz HC, Buss S, Andrassy M, Öttl R, Pfitzer G, Katus HA, Kaya Z. Mucosal tolerance induction in autoimmune myocarditis and myocardial infarction. *Int J Cardiol*. 2013;162:245–252. doi: 10.1016/j.ijcard.2011.05.057
17. Li J, Maguy A, Duverger JE, Vigneault P, Comtois P, Shi Y, Tardif J-C, Thomas D, Nattel S. Induced KCNQ1 autoimmunity accelerates cardiac repolarization in rabbits: potential significance in arrhythmogenesis and antiarrhythmic therapy. *Heart Rhythm*. 2014;11:2092–2100. doi: 10.1016/j.hrthm.2014.07.040
18. Quang KL, Maguy A, Qi X-Y, Naud P, Xiong F, Tadevosyan A, Shi Y-F, Chartier D, Tardif J-C, Dobrev D, et al. Loss of cardiomyocyte integrin-linked kinase produces an arrhythmogenic cardiomyopathy in mice. *Circ Arrhythm Electrophysiol*. 2015;8:921–932. doi: 10.1161/CIRCEP.115.001668
19. Mitchell GF, Jeron A, Koren G. Measurement of heart rate and Q-T interval in the conscious mouse. *Am J Physiol*. 1998;274:H747–H751. doi: 10.1152/ajpheart.1998.274.3.H747
20. Boukens BJ, Rivaud MR, Rentschler S, Coronel R. Misinterpretation of the mouse ECG: "musing the waves of Mus musculus." *J Physiol*. 2014;592:4613–4626. doi: 10.1113/jphysiol.2014.279380
21. Berul CI, Christe ME, Aronovitz MJ, Seidman CE, Seidman JG, Mendelsohn ME. Electrophysiological abnormalities and arrhythmias in alpha MHC mutant familial hypertrophic cardiomyopathy mice. *J Clin Invest*. 1997;99:570–576. doi: 10.1172/JCI119197
22. Verheule S, Sato T, Everett T, Engle SK, Otten D, Rubart-von der Lohe M, Nakajima HO, Nakajima H, Field LJ, Olgin JE. Increased vulnerability to atrial fibrillation in transgenic mice with selective atrial fibrosis caused by overexpression of TGF-beta1. *Circ Res*. 2004;94:1458–1465. doi: 10.1161/01.RES.0000129579.59664.9d
23. McCauley MD, Hong L, Sridhar A, Menon A, Perike S, Zhang M, da Silva IB, Yan J, Bonini MG, Ai X, et al. Ion channel and structural remodeling in obesity-mediated atrial fibrillation. *Circ Arrhythm Electrophysiol*. 2020;13:e008296. doi: 10.1161/CIRCEP.120.008296
24. Huber W, von Heydebreck A, Sültmann H, Poustka A, Vingron M. Variance stabilization applied to microarray data calibration and to the quantification of differential expression. *Bioinformatics*. 2002;18(suppl 1):S96–S104. doi: 10.1093/bioinformatics/18.suppl_1.s96
25. Lemme M, Ulmer BM, Lemoine MD, Zech ATL, Flenner F, Ravens U, Reichenspurner H, Rol-Garcia M, Smith G, Hansen A, et al. Atrial-like engineered heart tissue: an in vitro model of the human atrium. *Stem Cell Rep*. 2018;11:1378–1390. doi: 10.1016/j.stemcr.2018.10.008
26. Sheng X, Reppel M, Nguemo F, Mohammad FI, Kuzmenkin A, Hescheler J, Pfannkuche K. Human pluripotent stem cell-derived cardiomyocytes: response to TTX and lidocain reveals strong cell to cell variability. *PLoS One*. 2012;7:e45963. doi: 10.1371/journal.pone.0045963
27. Zhao Z, Lan H, El-Battrawy I, Li X, Buljubasic F, Sattler K, Yücel G, Lang S, Tiburcy M, Zimmermann W-H, et al. Ion channel expression and characterization in human induced pluripotent stem cell-derived cardiomyocytes. *Stem Cells Int*. 2018;2018:6067096. doi: 10.1155/2018/6067096
28. Kovoor P, Wickman K, Maguire CT, Pu W, Gehrmann J, Berul CI, Clapham DE. Evaluation of the role of I(KACh) in atrial fibrillation using a mouse knockout model. *J Am Coll Cardiol*. 2001;37:2136–2143. doi: 10.1016/s0735-1097(01)01304-3
29. Tuomi JM, Chidiac P, Jones DL. Evidence for enhanced M3 muscarinic receptor function and sensitivity to atrial arrhythmia in the RGS2-deficient mouse. *Am J Physiol Heart Circ Physiol*. 2010;298:H554–H561. doi: 10.1152/ajpheart.00779.2009
30. Tuomi JM, Tyml K, Jones DL. Atrial tachycardia/fibrillation in the connexin 43 G60S mutant (oculodentodigital dysplasia) mouse. *Am J Physiol Heart Circ Physiol*. 2011;300:H1402–H1411. doi: 10.1152/ajpheart.01094.2010
31. Zhou Y, Xu W, Han R, Zhou J, Pan Z, Rong H, Li J, Xu C, Qiao G, Lu Y. Matrine inhibits pacing induced atrial fibrillation by modulating I(KM3) and I(Ca-L). *Int J Biol Sci*. 2012;8:150–158. doi: 10.7150/ijbs.8.150
32. Nattel S, Maguy A, Le Bouter S, Yeh Y-H. Arrhythmogenic ion-channel remodeling in the heart: heart failure, myocardial infarction, and atrial fibrillation. *Physiol Rev*. 2007;87:425–456. doi: 10.1152/physrev.00014.2006
33. Nattel S, Burstein B, Dobrev D. Atrial remodeling and atrial fibrillation: mechanisms and implications. *Circ Arrhythm Electrophysiol*. 2008;1:62–73. doi: 10.1161/CIRCEP.107.754564
34. Ehrlich JR. Inward rectifier potassium currents as a target for atrial fibrillation therapy. *J Cardiovasc Pharmacol*. 2008;52:129–135. doi: 10.1097/FJC.0b013e31816c4325
35. Van Wagoner DR, Pond AL, McCarthy PM, Trimmer JS, Nerbonne JM. Outward K+ current densities and Kv1.5 expression are reduced in chronic human atrial fibrillation. *Circ Res*. 1997;80:772–781. doi: 10.1161/01.res.80.6.772
36. Dobrev D, Friedrich A, Voigt N, Jost N, Wettwer E, Christ T, Knaut M, Ravens U. The G protein-gated potassium current I(K,ACh) is constitutively active in patients with chronic atrial fibrillation. *Circulation*. 2005;112:3697–3706. doi: 10.1161/CIRCULATIONAHA.105.575332
37. Cha T-J, Ehrlich JR, Chartier D, Qi X-Y, Xiao L, Nattel S. Kir3-based inward rectifier potassium current: potential role in atrial tachycardia remodeling effects on atrial repolarization and arrhythmias. *Circulation*. 2006;113:1730–1737. doi: 10.1161/CIRCULATIONAHA.105.561738

38. Voigt N, Maguy A, Yeh Y-H, Qi X, Ravens U, Dobrev D, Nattel S. Changes in I K, ACh single-channel activity with atrial tachycardia remodelling in canine atrial cardiomyocytes. *Cardiovasc Res*. 2008;77:35–43. doi: 10.1093/cvr/cvm051
39. Makary S, Voigt N, Maguy A, Wakili R, Nishida K, Harada M, Dobrev D, Nattel S. Differential protein kinase C isoform regulation and increased constitutive activity of acetylcholine-regulated potassium channels in atrial remodeling. *Circ Res*. 2011;109:1031–1043. doi: 10.1161/CIRCRESAHA.111.253120
40. Hibino H, Inanobe A, Furutani K, Murakami S, Findlay I, Kurachi Y. Inwardly rectifying potassium channels: their structure, function, and physiological roles. *Physiol Rev*. 2010;90:291–366. doi: 10.1152/physrev.00021.2009
41. Guasch E, Benito B, Qi X, Cifelli C, Naud P, Shi Y, Mighiu A, Tardif J-C, Tadevosyan A, Chen Y, et al. Atrial fibrillation promotion by endurance exercise: demonstration and mechanistic exploration in an animal model. *J Am Coll Cardiol*. 2013;62:68–77. doi: 10.1016/j.jacc.2013.01.091
42. Wehrens XHT, Chiang DY, Li N. Chronic exercise: a contributing factor to atrial fibrillation? *J Am Coll Cardiol*. 2013;62:78–80. doi: 10.1016/j.jacc.2013.02.070
43. Liang KP, Kremers HM, Crowson CS, Snyder MR, Therneau TM, Roger VL, Gabriel SE. Autoantibodies and the risk of cardiovascular events. *J Rheumatol*. 2009;36:2462–2469. doi: 10.3899/jrheum.090188
44. Chan CT, Lieu M, Toh B-H, Kyaw TS, Bobik A, Sobey CG, Drummond GR. Antibodies in the pathogenesis of hypertension. *Biomed Res Int*. 2014;2014:504045. doi: 10.1155/2014/504045
45. Iseme RA, McEvoy M, Kelly B, Agnew L, Walker FR, Handley T, Oldmeadow C, Attia J, Boyle M. A role for autoantibodies in atherogenesis. *Cardiovasc Res*. 2017;113:1102–1112. doi: 10.1093/cvr/cvx112
46. Danielson KM, Das S. Extracellular vesicles in heart disease: excitement for the future? *Exosomes Microvesicles*. 2014;2:10.5772/58390. doi: 10.5772/58390
47. Sluijter JPG, Verhage V, Deddens JC, van den Akker F, Doevendans PA. Microvesicles and exosomes for intracardiac communication. *Cardiovasc Res*. 2014;102:302–311. doi: 10.1093/cvr/cvu022
48. Doyle LM, Wang MZ. Overview of extracellular vesicles, their origin, composition, purpose, and methods for exosome isolation and analysis. *Cells*. 2019;8:727. doi: 10.3390/cells8070727
49. Shen B, Wu N, Yang J-M, Gould SJ. Protein targeting to exosomes/microvesicles by plasma membrane anchors. *J Biol Chem*. 2011;286:14383–14395. doi: 10.1074/jbc.M110.208660
50. Corey S, Krapivinsky G, Krapivinsky L, Clapham DE. Number and stoichiometry of subunits in the native atrial G-protein-gated K+ channel, IKACh. *J Biol Chem*. 1998;273:5271–5278. doi: 10.1074/jbc.273.9.5271
51. Arora R, Ng J, Ulphani J, Mylonas I, Subacius H, Shade G, Gordon D, Morris A, He X, Lu Y, et al. Unique autonomic profile of the pulmonary veins and posterior left atrium. *J Am Coll Cardiol*. 2007;49:1340–1348. doi: 10.1016/j.jacc.2006.10.075
52. Fu F, Pietropaolo M, Cui L, Pandit S, Li W, Tarnavski O, Shetty SS, Liu J, Lussier JM, Murakami Y, et al. Lack of authentic atrial fibrillation in commonly used murine atrial fibrillation models. *PLoS One*. 2022;17:e0256512. doi: 10.1371/journal.pone.0256512
53. Felix SB, Beug D, Dörr M. Immunoadsorption therapy in dilated cardiomyopathy. *Expert Rev Cardiovasc Ther*. 2015;13:145–152. doi: 10.1586/14779072.2015.990385